DOI: 10.15587/978-617-8360-17-7.CH4

Oleg Shinsky, Inna Shalevska, Iuliia Kvasnytska,
Pavlo Kaliuzhnyi, Oleksandr Neima, Anatolii Shalevskyi

4 CAST STRUCTURES WITH COMPOSITE AND REINFORCED NON-METALLIC FUNCTIONAL FILLER

ABSTRACT

The chapter presents the results of research on the scientific and technological prerequisites for obtaining steel hollow castings with composite and reinforced non-metallic filler by the lost foam casting method.

A system of equations was obtained that describes the gas-hydrodynamic conditions of lost foam casting with polystyrene patterns saturated with reinforcing elements (RE), and taking into account the heat exchange between RE and the matrix melt during mold filling and casting solidification.

Modern domestic and foreign materials for cast structures for protective purposes were analyzed and the prospects for the use of low-alloy and microalloyed steels were determined. It was established that optimal performance characteristics are achieved under the conditions of the correct selection of heat treatment modes, which provides a combination of high strength with sufficient plasticity.

To determine the influence of composite and non-metallic fillers on the possibility of obtaining a high-quality casting, computer simulation methods were used and the results obtained were verified by full-scale experiments.

The research conducted by the authors at the Physico-Technological Institute of Metals and Alloys of the National Academy of Sciences of Ukraine and carried out within the framework of project No. 2023.04/0029, state registration 0124U003980, supported by a grant from the National Research Foundation of Ukraine under the program "Science for Strengthening the Defense Capability of Ukraine" is of high scientific and practical importance for the manufacture of special-purpose foundry products and will be useful for specialists-manufacturers of foundry, scientists and scientific and pedagogical workers in the specialty "Metallurgy" (Foundry).

KEYWORDS

Reinforced cast structure, reinforcing filler, matrix melt, gas-hydrodynamic conditions, heat exchange processes, computer simulation, polystyrene foam pattern, cast steel, alloying, lost foam casting, heat treatment of steel, technological process.

Modern foundry production today is focused on a significant reduction in the metal content of products, simultaneously with the complication of their geometry and functional purpose. Therefore, the creation of scientifically based new technologies for the manufacture of hollow steel structures with special

properties by the method of lost foam casting using reinforcing fillers is relevant and required additional research into the processes of heat and mass transfer and gas-hydrodynamics and the determination of optimal technological parameters.

To implement in industry a new design of cast hollow steel modules with a spherical surface and high-hardness compacted fillers and metal composites with a steel shell, the technology of lost foam casting was adapted, which made it possible to obtain a given binary design of modules of the system "steel shell — compacted filler in a bound state" and "steel shell — reinforced metal composite" in a single-cycle technological process and directly in the mold.

The new technological process for producing cast binary modules is based on the use of polystyrene foam patterns filled with the specified dispersed materials, which are installed in a mold, in which a vacuum is created and directly in the presence of the pattern, the liquid metal of the shell is poured. Under the conditions of heat exchange between the liquid metal and the polymer pattern, the latter undergoes thermal destruction, and its volume is filled with liquid metal. Under the influence of the heat flow from the metal, the filler forms a solid material in the form of a metal composite with a reinforcing steel phase, which corresponds in chemical composition to the shell metal. In this case, the liquid metal seeps into the filler due to the pressure gradient between the metal P_m and the porous filler P_f (P_m—P_f), since a vacuum is formed in the latter within (0.1...0.2) P_a (P_a — atmospheric pressure).

4.1 DETERMINATION OF THE THERMOPHYSICAL MODEL OF THE INTERACTION OF THE REINFORCING FILLER AND THE STEEL MATRIX MELT IN THE MOLD

The production of reinforced castings by lost foam casting are accompanied by complex gas-hydrodynamic and heat-mass exchange processes. When obtaining hollow castings by reinforcing them with metal and non-metallic fillers located in polystyrene foam patterns, new multi-component systems arise for the theory of casting processes: "metal — pattern — filler — mold" and "metal — reinforcing filler — mold". Therefore, the study of the regularities of heat and mass exchange in these systems in the manufacture of shell binary cast structures and their mathematical description is relevant. In this case, it is necessary to determine the influence of the presence of solid and porous polystyrene foam patterns, metal and non-metallic materials in the mold on the conditions of heat exchange in the mold. The phenomenon of liquid flow during lost foam casting is essentially a problem of unsteady flow with free boundaries. Molten metal flowing in the mold during lost foam casting destroys the polystyrene foam pattern, forming a gas gap between the molten metal and the pattern. The rate of destruction of the pattern and the pressure in this gap depend on the heat exchange in the mold, and in the presence of reinforcing elements this process is complicated. There is information on the development of a two-dimensional thermal model, which is based on the mass and energy balance in the gas gap between the polystyrene foam pattern and the molten metal. The pressure in the gap is determined by the mass and energy balance method, which directly takes into account such important process parameters as the permeability of the coating, foam characteristics, pouring temperature and metal properties, but does not take into account the presence of additional reinforcement [1].

Therefore, research devoted to the development of a thermophysical model of the interaction of the reinforcing filler, polystyrene foam pattern and liquid steel in the mold during lost foam casting was relevant.

At the same time, the development of a thermophysical model of the interaction of the reinforcing filler, liquid steel and polystyrene foam pattern in the mold during lost foam casting will make it possible to predict the conditions of the melt flow, its solidification and cooling in the mold, which makes it possible to create promising casting methods for obtaining high-quality reinforced structures, including hollow binary modules for protective structures.

The authors established the conditions of heat exchange in the mold in which the reinforcing elements are placed, under different flow regimes of the matrix alloy in the porous channels of the polystyrene foam pattern.

The process of interaction of molten metal with mono- and reinforced polystyrene foam pattern during lost foam casting was investigated.

According to previously established laws on the conditions of casting solidification, movement of matrix alloy (MA) in the mold in the presence of metal reinforcing elements (RE), their interaction with the polystyrene foam pattern and thermal destruction products in the form of liquid, gaseous and solid phases, a physical model of mass and heat transfer was developed during the formation of the structure and properties of cast reinforced structures in multicomponent systems new to the theory of casting processes: "metal – pattern – RE – mold" [2, 3].

At the same time, the boundary temperature conditions and the final temperature at the heat exchange boundary of the "MA-RE" system were established

$$T_k = \frac{T_L - T_S}{2}, \tag{4.1}$$

where T_L, T_S – liquidus and solidus temperatures for the matrix alloy, °C.

For the integrated MA-RE system, the heat exchange contact area will be $n.S_P$, $n.S_{MRE}$, respectively, where n –the number of reinforcing elements located in the mold cavity, pcs., and their mass will be

$$m = 0.785 \cdot n \cdot g_{MRP} \cdot R^2_{MRP} \cdot L_{MRP}, \text{ kg} \tag{4.2}$$

where g_{MRP} – density, kg/m^3; L_{MRP} – characteristic length of the reinforcing element, m.

It should be noted that the vertical reinforcing elements installed in the mold (in this case, it is possible to consider them in the form of rods) complicate the flow area of the liquid metal (mold) and have a certain effect on the thermophysical and hydrodynamic processes occurring in it.

When obtaining castings, the resistance of the filler metal medium to be poured depends on the temperature conditions of filling the mold, the dimensions and geometry of the reinforcing elements and their placement in the mold cavity. It should be noted that the liquid alloy with dense packing of RE flows through "capillary" thin channels, which are formed by particles of these elements or in the cavity of the mold, in which RE are located at a fixed distance from each other.

To simplify the problem, it is possible to use the conditions of heat exchange in the form of a limit in a single channel of length L, filled with rods according to the heat balance scheme presented in works [3, 4] and in **Fig. 4.1, *a***, and has the form

$$c_p \cdot \rho \cdot V_{cp} \cdot F_c \cdot \left(T_{b_1} - T_{b2}\right) = \alpha_c \cdot F_n \cdot \left(T_c - T_b\right)_c, \quad (4.3)$$

where T_{b2} – the average temperature at the channel outlet over the channel cross section, °C;

T_{b1} – the average temperature at the channel inlet over the channel cross section, °C;

C_p – the specific heat capacity, J/(kg×°C);

ρ – the MA density, kg/m^3;

F_c – the cross-sectional area of a single capillary channel, m^2;

V_c – the average flow velocity in the channel, m/s;

F_n – the total contact area of the liquid metal with the surface of the channel (filler), m^2;

T_c – the average wall temperature along the channel length, °C;

T_b – respectively, the average temperature of the liquid alloy along the channel length, °C;

α_c – the heat transfer coefficient at the boundary of the porous channel formed between the RE and the MA melt, W/m^2,°C.

It is also recommended to determine the heat transfer coefficient by formulas, the structure of which depends on the MA flow regime in the pore channels (laminar or turbulent) [4]. At the same time, for practical use and study of the kinetics of changes in the temperature of the matrix melt in the pore space, it is recommended to represent the contact surface of heat exchange in the system "matrix melt – reinforced phase" through the equivalent (integral) radius of the reinforcing element R_{ae} [2]. In this case, the heat transfer coefficient for the MA laminar flow in the channels formed by the RE is determined by the equation of the dimensionless heat transfer coefficient Nu_D [4]

$$Nu_{\overline{D}} = \frac{\alpha_c \overline{D}}{\lambda_c} = 1.86\left(\mathrm{Re}_{\overline{D}} \cdot \mathrm{Pr}\right)^{0,33} \cdot \left(\frac{\overline{D}}{L}\right)^{0,33} \cdot \left(\frac{\mu_b}{\mu_s}\right)^{0,14}, \quad (4.4)$$

where $\overline{D}$ – the given channel diameter, m;

λ_c – Nusselt criterion, which characterizes the similarity of heat transfer processes at the interface between the wall and the fluid flow;

$\mathrm{Pr} = \frac{\nu}{a}$ – Prandtl criterion;

$\mathrm{Re} = \frac{V \cdot \overline{D}}{\nu}$ – Reynolds criterion;

n – viscosity coefficient, m^2/s;

α_c – thermal diffusivity coefficient, m^2/s;

μ_b – dynamic viscosity at metal temperature T_b, H×s/m^2;

μ_c – dynamic viscosity at wall temperature T_s(T_s^3 T_L);

T_L – liquidus temperature of the matrix alloy °C.

For turbulent MA flow regime in RE porous channels, the formula for *Nu* is recommended

$$Nu_{\overline{D}} = \frac{\alpha_c \cdot \overline{D}}{\lambda_c} = 0{,}036 \cdot \mathrm{Re}_D^{0{,}8} \cdot \mathrm{Pr}^{0{,}33} \cdot \left(\frac{\overline{D}}{L}\right)^{0{,}055}, \quad (4.5)$$

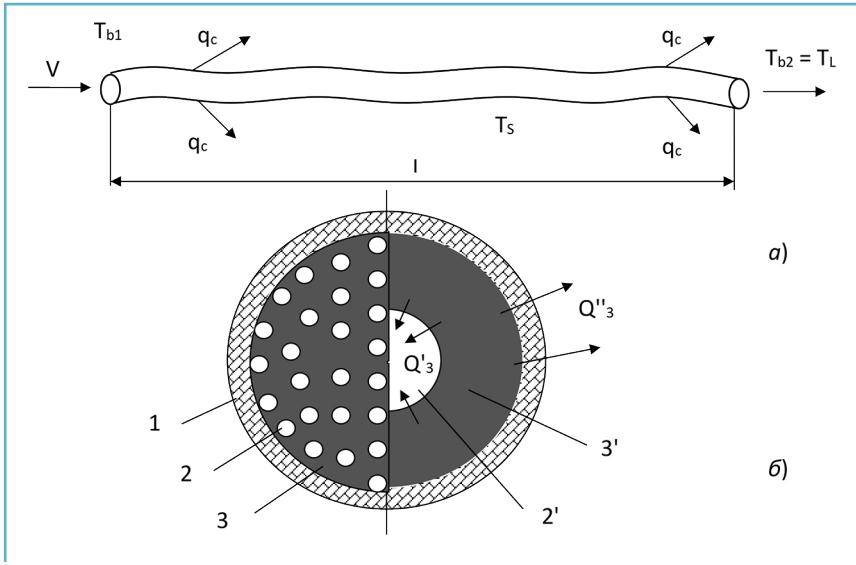

Fig. 4.1 Heat exchange scheme during melt flow in the pore space of the reinforcing phase along: a - the length; b - the cross-section of the mold with RE oriented in it: (*b*): 1 — shell (mold); 2 — reinforcing element; 3 — matrix melt; 2′ — equivalent cross-section of the reinforcing element; 3′ — equivalent cross-section of the matrix melt
Source: [3]

However, despite the achievements in the theory of MA melt flow in the RE environment located in the cavity of the mold, in the theory of lost foam casting the features of the interaction of thermal destruction products of the gasified pattern (GP) and their influence on the gasohydrodynamics of the process and the formation of the quality of cast blanks in the absence of a macroreinforcing phase were more often considered.

The RE presence directly in the polystyrene GP, and the latter is located in the cavity of the mold, allows to change the conditions of filtration and mass transfer of vapor-gas (VGP) and liquid products (LP), which are formed during the destruction of the pattern and modify the gas dynamics of the process, as well as the conditions for forming the quality of castings.

The features of VGP filtration through the known system: " VGP — coating — mold" and the new "VGP RE channel — GP — coating — mold" were considered, taking as a basis the physical model of the process of filling the mold with GP with "zero" open porosity, which is presented in the works [2, 5].

When filling the mold through the gap "metal — pattern" and channels around the reinforcing elements, the GP undergoes the VGP filtration process. During the mold pouring with liquid MA 1 (**Fig. 4.2**) at a speed W_1, the GP decomposes at a linear speed W_5, and since $W_1 < W_5$, a "meta l- pattern" gap d_1 is formed, in which a backpressure R_f is formed due to the VGP formation. At the same time, the LP covers the entire surface of the MA flow front in the form of a thin film "*D*" [6]. The heat flux from the liquid MA to the GP is transmitted by radiation and thermal conductivity through the LP film "*D*" and the gas-saturated gap "*d*". In this case, the heat exchange surface on the side of the pattern F_5 is reduced by the area of the RE F_a compared to the monopattern. In addition, part of the pattern destruction products at the time of the formation of the gap d_1 is filtered in the VGP form into the depth of the mold under the action of the P_f–P_a pressure gradient, first through the refractory coating (RC) 2 and accumulates on the grains of the molding material (MM) 4 in the form of a condensed liquid phase (CLP).

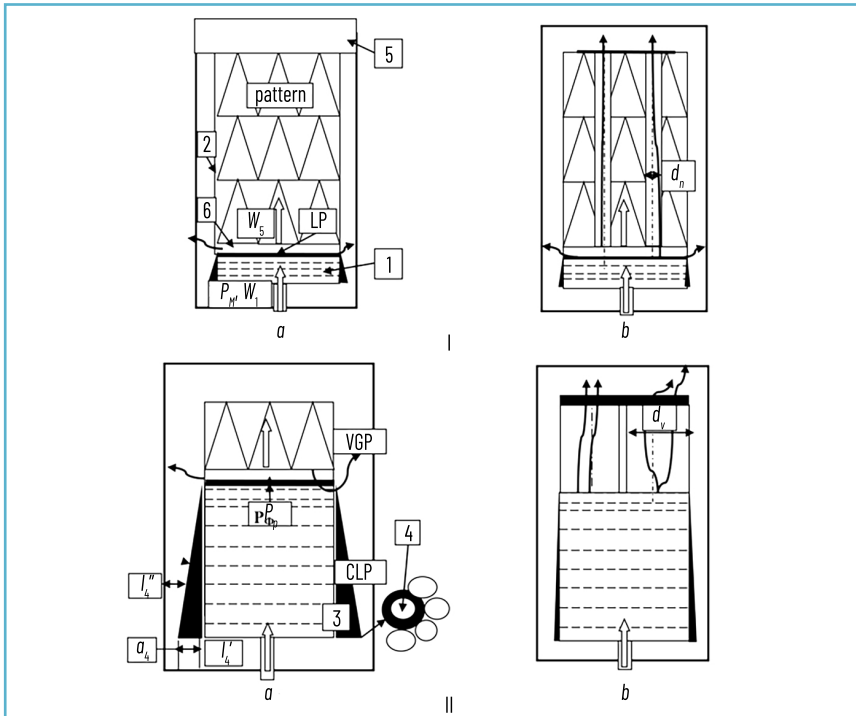

Fig. 4.2 Physical model of the interaction of a gasified pattern with metal during the period of filling the mold with: a - a mono pattern; b - reinforced pattern: 1 — metal; 2 — refractory coating on the-pattern; 3 — zone of low gas permeability (LGP); 4 — molding material (MM); 5 — mold; 6 — gap "metal — pattern"; products of thermal destruction of polystyrene: LP — liquid, VGP — vapor-gas; CLP — VGP condensate on MM grains; P_p, P_m — VGP pressure in the gap and metal, respectively; W_1, W_5 — linear velocity of destruction of the pattern and metal rise in the mold; I — initial stage of pouring, II — final stage of pouring
Source: [3]

At the same time, a zone of low gas permeability 3 (LGP) with a width of a_4 is formed at a distance of l_4 from the "metal- mold" boundary due to partial CLP overlap of the MM channels. In this case, the VGP flow passes through four zones in the mold: RC with a thickness d and gas permeability K_p, two MM layers with a thickness $l_{4'}$ and $l_{4''}$ and gas permeability $K_{4'}$ and LGP with a width of a^4 with gas permeability K_{LGP}.

In the same period, when the mold is filled with MA, VGP is also filtered through channels with a diameter d_n–d_g, which formed around the RE by GP thermal destruction due to temperature exchange between the RE and the GP. At the same time, a new heat exchange system is also formed: "GP (VGP) – RE (pore channels)", which leads to additional GP thermal destruction and an increase in the channel diameter to the value d_y [2].

In this case, the VGP is filtered through the channel with an area F_d and the RC into the mold wall with the formation of a similar LGP. Under the action of the pressure gradient (P_p–P_y), the LP formation in a mixture with VGP is carried to the end surface of the mold, and does not accumulate in the pore channel or on the surface of the metal flow front.

Based on the presented physical model of VGP filtration in the mold, the kinetics of the change in the gas regime during the lost-foam casting (LFC) process was described using the well-known system of equations (6), which is presented in works [3, 5]

$$\begin{cases} \dfrac{dy}{d\tau} = \dfrac{\left(\dfrac{\alpha\Delta T}{r\rho_5(1+N)} - \left(1-\dfrac{\delta}{\delta_c}\right) + \dfrac{\lambda\Delta T}{\delta r\rho_5(1+N)}\right)}{\left(1+\dfrac{\alpha\Delta T}{r\rho(1+N)} - \dfrac{\rho_5\tau\left(1-\delta/\delta_0\right)}{y'(1+M_G\tau)\rho_c\left[\left(\delta/\tau W_1\right)^{0.05}\right]}\right)} - W_1, \\ \dfrac{dQ}{d\tau} = W_5\rho_5 m_G V_G F_5(1-\varphi) - \delta P_5 P_f K_4 \varphi_G \left[\dfrac{c\left(l_4' - l_4''\right) + a_4}{\left(l_4' + l_4''\right)a_4}\right], \\ c = 0.0014 \cdot \dfrac{r \cdot m_G \cdot \rho_5 \cdot R_5}{a_4}, l_4' = (3.2 - 0.012T_3)\tau, \\ a_4 = 0.015T_3, \varphi = 0.32 \cdot K_p^{1/3}, P_{\varphi i} = \dfrac{PQ}{F_5\delta}, \end{cases} \quad (4.6)$$

where α – heat transfer coefficient, W/(m^{2}K);

ρ_5 – pattern density;

ρ_p – liquid phase density, kg/m^3;

t – time, s;
y' – thickness of spheroids P_p, m;
ΔT – temperature difference between metal and melting pattern, K;
V_g – specific VGP volume, m^3/kg;
λ – thermal conductivity coefficient of vapor-gas phase, W/(m×K);
r – heat of fusion of pattern material, J/kg;
N – melting criterion;
δ – gap, m;
δ_0 – gap at which $W_5 < W_1$, m;
M_r – degree of destruction;
φ – accumulation of liquid GP products;
F_5 – cross-sectional area of pattern (casting), m^2;
P_5 – perimeter of pattern (casting) cross-section, m;
K_4 – gas permeability of the molding material, m^2/(N s);
K_p – gas permeability of the coating, units;
l_4', l_4'' – length of the molding material layer, m;
a_4 – LGP width, m;
φ_g – gas permeability reduction coefficient;
Q – VGP volume, m^3;
P_f – pressure in the gap, Pa;
T_3 – temperature of the alloy being poured, K;
τ_1 – time from the moment of pouring the metal into the mold, s.

Given that the GP has pore channels around the reinforcing elements with an area of ΣF_d, then the contact area of the heat flow of the metal with the GP F_k can be represented by the following equations (4.7)–(4.9)

$$F_K = F_5 - \sum_{i=1}^{i=n} F_i, m^2 \tag{4.7}$$

or

$$F_K = F_5 - \xi F_5, \quad \xi = \frac{\sum_{i-1}^{i=n} F_i}{F_5}, m^2 \tag{4.8}$$

and finally

$$F_K = (1-\xi)F_5, m^2 \tag{4.9}$$

where F_k; F_5; F_i – area of thermal contact, monopattern and pore channels around RE, respectively, m^2; ξ – porosity degree of the pattern.

As a result of the formation of a new VGP filtration system, namely: "VGP – reinforced phase – pore channels – coating –mold", the total VGP filtration area can be determined by the following mathematical dependence (4.10)

$$F_{\Sigma} = \left(\delta\Pi_5 + \xi F_5\right), m^2. \tag{4.10}$$

At the same time, the cross-sectional area of the elementary pore channel F_i is a variable value, because under the action of heating its VGP contact surface, the GP material around the RE decomposes at a speed a_5', which leads to an increase in its diameter d_i. The change in the total area of the GP channels can be described by the following expression, assuming that the channels have a cylindrical shape (4.11), (4.12) [3]:

$$\sum F_i' = \sum_{i=1}^{i=n} \frac{\pi d_\tau^{\,2}}{4}, m^2 \tag{4.11}$$

$$d_\tau = \left(1 + 2a_5' T_G\right) d_n, \tag{4.12}$$

where d_n – the initial diameter of the elementary pore channel, equal to the diameter of the reinforcing element d_a, m;

d_τ – the current diameter of the elementary pore channel around the reinforcing element, m;

a_5 – the linear melting velocity of the GP in the pore channel, m/s;

T_g – the VGP temperature, K;

τ – the current pouring time, s.

In order to use equations (4.11), (4.12) in the mathematical model (4.6), the following transformations should be performed, namely (4.13):

$$\frac{\xi_\tau}{\xi_n} = \frac{\left(d_n + 2a_5' T_G \cdot \tau\right)^2 4\pi}{4\pi d_n^{\,2}}, \tag{4.13}$$

and finally, the variable porosity (14):

$$\xi_\tau = \frac{\left(d_n + 2a_5' T_G \tau\right)^2}{d_n^{\,2}} \cdot \xi_n. \tag{4.14}$$

In this case, the system of equations of the gas dynamics of the casting process in the presence of GP with RE in the mold has the following form (4.15):

$$\begin{cases} \dfrac{dy}{d\tau} = \dfrac{\left(\dfrac{\alpha\Delta T}{r\rho_5(1+N)} - \left(1-\dfrac{\delta}{\delta_0}\right) + \dfrac{\lambda\Delta T}{\delta r\rho_5(1+N)}\right)}{\left(1+\dfrac{\alpha\Delta T}{r\rho_5(1+N)} - \dfrac{\rho_5\tau\left(1-\dfrac{\delta}{\delta_0}\right)}{y'(1+M_6\tau)\rho_{c_{-p}}\left[\left(\dfrac{\delta}{\tau W_1}\right)^{0.05}\right]}\right)} - W_1, \\ \dfrac{dQ}{d\tau} = (1-\xi_\tau)F_5W_5\rho_5M_6a_5(1-\varphi) - \\ -\left(\delta P_5 + \dfrac{\left(d_n + 2a_5'T_6\tau\right)^2}{d_n^2}\cdot F_5\right)\varphi_\Gamma\Delta\rho K_4\dfrac{L_\Sigma - c\left(l_4' - l_4''\right)}{\left(l_4' - l_4''\right)a_4}, \\ P_{\varphi i} = \dfrac{PQ}{F_5\delta}, L = (3.2-0.012T_3)\cdot\tau_3, a_4 = 0.015T_3, \varphi_\Gamma = 0.32\cdot K^{1/3}, a_5' = 1\cdot10^{-3}. \end{cases} \quad (4.15)$$

To determine the coefficient, it is possible to use the data of work [7] and construct the dependence $d = f(T_g)$, where d – the diameter of the pore channel, and T_g – the temperature of the gas passing through this channel. According to the graph (**Fig. 4.3**), this dependence is expressed by a straight line. In this case, the equation for determining the coefficient a_5' has the following form (4.16)

$$a_5' = \frac{\Delta d}{2\Delta T_6\cdot 10}, \quad (4.16)$$

where 10 is the time of gas passage through the pore channel of the GP in the experiment, C.

Then the value of the coefficient is $a_5' = 1\times10^{-3}$ mm/s °C.

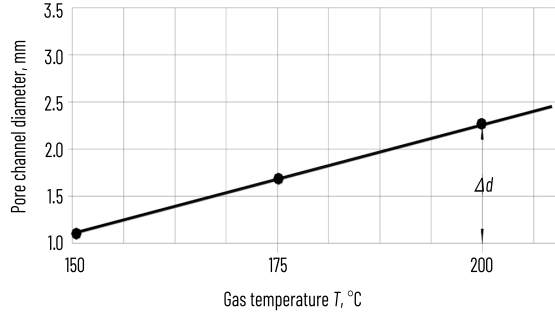

Fig. 4.3 Kinetics of change in linear dimensions of the pore channel in the polystyrene foam pattern

Now the system of equations (4.15) can be used to determine the parameters, including the back pressure of the VGP P_p, the gap "metal – pattern" δ and the rate of metal rise in the mold W_1 with a reinforced GP.

It is also important to note that the amount of LP products that accumulate on the surface of the metal flow front is also reduced by the value $(F_5 - \Sigma F_d)$. In this case, to determine the volume of LP accumulation, the time of its gasification on the contact surface for time t_g and the hardening coefficient R, it is advisable to use the system of equations (4.15) by supplementing it with the expression $\left(1-\xi_\tau\right)F_5$.

Then the system of equations describing the gas-hydrodynamic conditions of lost foam casting with polystyrene patterns saturated with RE, and taking into account the heat exchange between the RE and the MA during mold filling and matrix alloy solidification, has the final form (4.17):

$$
\begin{cases}
P_p = 0.13\varphi_G \dfrac{\eta T_p I_4}{c} a_5 t_G^{\,m-1}, \\
\xi_1 = \dfrac{1.13 b_4 \left(T_p - T_m\right) \cdot \left[1 + \dfrac{100\left(1-c_\tau\right)^3 \delta_1 3}{1.13 b_4 \left(T_p - T_m\right)}\right]}{L_1 \rho_1 \left[1 - \dfrac{c_1}{L_1}\left(T_3 - T_{kp}\right)\right]} \cdot \sqrt{t_G}, \\
C_\tau = \dfrac{\left(d_n + 2a_5^{'} \cdot T_G \cdot \tau\right)^2}{d_n^2}, \\
P_M = \rho_1 g_1 W_1 t_G, \\
t_G = \left(\dfrac{\left(1-c_\tau\right)^3 \delta_1^{\,3}}{a_5} \cdot 10^3\right)^{\frac{1}{m}}, \\
\begin{cases}
\tau = \dfrac{C_p \rho_1 V_c \sqrt{\xi} \cdot D_1}{\alpha_{-}\left(T_{-} - \left[T_1\right]\right)}, \\
\left(T_c - \left[T\right]\right)_c = \left(\dfrac{T_3 + \left[T_1\right]}{2} - \left[T_1 + KpP_5 / 25\right]\right),
\end{cases} \\
Nu_{\overline{D}} = \dfrac{\alpha_c \overline{D}}{\lambda_c} = 1.86\left(\mathrm{Re}_{\overline{D}} \cdot \mathrm{Pr}\right)^{0.33} \cdot \left(\dfrac{\overline{D}}{L}\right)^{0.33} \cdot \left(\dfrac{\mu_b}{\mu_s}\right)^{0.14}, \\
Nu_{\overline{D}} = \dfrac{\alpha_c \cdot \overline{D}}{\lambda_c} = 0.036 \cdot \mathrm{Re}_D^{\,0.8} \cdot \mathrm{Pr}^{0.33} \cdot \left(\dfrac{\overline{D}}{L}\right)^{0.055}.
\end{cases}
\tag{4.17}
$$

where η – the coefficient of VGP dynamic viscosity;

T_p – the metal temperature, K;

T_m – the mold temperature, K;

C – the permeability, Darcy;

t_G – the gasification time of the pattern;

d_p – the diameter of the pore channel (reinforcing element);

φ_g – the SRC resistance coefficient;

b_4 – the heat storage capacity of the mold, W×s$^{0.5}$/m^2×K;

l_4 – the mold wall thickness, m;

D_1 – the diameter (reduced thickness) of the casting, m;

F_1, F_p – the cross-sectional area of the casting and the pore space, respectively, m^2;

ξ – the porosity coefficient of the mold;

λ_c – the thermal conductivity coefficient, W/(m×K);

$\mathrm{Pr} = \frac{\nu}{a}$ – Prandtl criterion;

$\mathrm{Re} = \frac{V \cdot \overline{D}}{\nu}$ – Reynolds criterion;

n – the viscosity coefficient, m^2/s;

α_c – the thermal diffusivity coefficient, m^2/s;

μ_b – dynamic viscosity at metal temperature T_b, N×s/m^2;

μ_c – dynamic viscosity at wall temperature T_s (T_s ^{3} T_L), N×s/m^2;

T_L – liquidus temperature of matrix alloy °C.

Thus, hydro-gas-dynamic, thermophysical models were created that describe the features of gas dynamics and heat and mass transfer in molds with reinforcing elements, a polystyrene foam pattern saturated with RE, which allow predicting the flow conditions of the matrix alloy, its solidification, and cooling in molds, which makes it possible to create promising casting methods using gasifying patterns to obtain high-quality reinforced structures with various functional properties from iron-carbon and non-ferrous alloys.

4.2 ANALYSIS AND SELECTION OF STEEL GRADES FOR THE MANUFACTURE OF HOLLOW CAST STRUCTURES FOR MULTIFUNCTIONAL PURPOSES

High requirements for the level of physical and mechanical properties of cast alloys, as well as the technological possibility of forming hollow castings with metallic and non-metallic reinforcing phases by lost foam casting, determine the feasibility of developing new high-strength economical alloyed steels. Such steels should provide the required set of operational properties without the use of scarce and expensive alloying elements, as well as contribute to the creation of highly efficient casting technologies and optimal heat treatment modes to obtain high-quality parts of protective structures [8–11].

Modern requirements for materials, in particular, for multifunctional protective structures, provide for a combination of high strength, sufficient plasticity and resistance to dynamic loads. The choice of material is a key factor determining the reliability and durability of structures manufactured by casting methods.

In this regard, there is a need for systematic research of alloys suitable for forming thin-walled castings of complex configuration [12].

For the analysis, domestic and foreign analogues of steels and iron-based alloys used in the production of cast structures were considered [13–15]. Based on the comparative analysis, it was established that among such materials, low- and medium-carbon low-alloy, microalloyed and modified steels have the greatest prospects. The urgent need for protective structures and structural requirements for their component modules – the level of physical and mechanical properties of steels, the possibility of manufacturing structural modules with non-metallic and metallic reinforcing phases (NRP and MRP) requires the development of new high-strength economically alloyed cast steels that do not contain expensive and scarce alloying elements, highly efficient technologies for manufacturing cast elements of a cellular structure and optimal modes of their heat treatment. A review of world analogues of steels used for the manufacture of multifunctional modules of protective structures has established that the steels used for their manufacture must provide a tensile strength of 500...950 MPa; yield strength – 450...800 MPa, relative narrowing 15...30%; impact toughness 50...70 J/cm2. In addition, given the great need for protective structures, steels for cast modules should not contain scarce and expensive alloying elements – nickel, molybdenum, copper, etc. An analysis of modern technical literature has established that for cast modules of protective structures, the required level of physical and mechanical properties of steels of the C-Si-Mn system is currently provided exclusively by their complex alloying with chromium, nickel, molybdenum, vanadium and the corresponding labor-intensive heat treatment regimes. Thus, regulatory documents for foundry steels in the USA – A352...A732 and Germany – DIN1681 provide for the manufacture of cast parts used as elements of protective structures, steels of the C-Si-Mn system, which are alloyed with the above chemical elements. This makes it possible, after appropriate heat treatment regimes, to obtain metal in products with a yield strength of over 400 MPa.

Based on previous studies [13], it can be stated that the processes of high-quality and optimal additional alloying, microalloying with carbide and nitride-forming elements and modification with nitrogen can achieve the required physical and mechanical properties (tensile strength at rupture 550...900 MPa, yield strength at rupture 450...750 MPa, relative elongation 15...30%, impact toughness 55...75 J/cm^2).

The physical and mechanical properties were determined and the microstructure of the experimental steels was considered using modern testing equipment and analytical methods. Special attention was paid to the influence of heat treatment modes on the operational characteristics of the metal, since energy consumption and stability of the properties of cast parts during mass production depend on this.

The blanks for samples for various purposes were manufactured in dry, heated sand-clay molds. To determine the mechanical properties, samples were made from blanks with a diameter of 12 mm and a length of 70 mm, to determine the impact toughness of steels, blanks with dimensions of 12 mm×12 mm×60 mm were cast, from which standard samples were made.

To compare the physical and mechanical properties and the results of metallographic studies, samples from blanks made using the tooling developed by us and cut from a tertiary blank in accordance with the requirements [14] were used.

To determine the impact toughness of the studied steels, blanks with dimensions of 12 mm×12 mm×60 mm were cast, from which standard samples were made.

To study other properties of steels (for example, choosing the optimal heat treatment regime for steels, studying the structure, etc.), cylindrical blanks with a diameter of 20 mm and a length of 90 mm and the lower part of the riser of the sprue system were used.

In order to determine the correctness of the choice of the tooling developed by us, a comparative assessment of the quality of the metal in the blanks made using the proposed tooling and made using a tertiary blank (DSTU 8781:2018, option 2) or a square (**Fig. 4.4, *a***). The metal has almost the same properties, but a complex test is more effective and much cheaper for the manufacture of samples from experimental steels (**Fig. 4.4, *b***). Obtaining high-quality metal in the samples using this technology is ensured by a massive boss under the riser.

a *b*

Fig. 4.4 Pattern tooling for the production of cast blanks: *a* — square, riser and tertiary blank; *b* — complex tooling (without riser)

The analysis of a large amount of material presented in the works of scientists of the Physico-Technological Institute of Metals and Alloys of the National Academy of Sciences of Ukraine on the use of alloying, microalloying and modification processes of C-Si-Mn alloys has identified specific areas for improving these processes for lost foam casting: approximate temperatures of base melts before performing the processes of additional alloying, microalloying and modification of base steels and pouring them into molds and specific individual chemical elements and complexes of elements to minimize their quantity with the maximum increase in the properties of experimental steels [15].

The studies have established that the optimal content of the main chemical elements in medium-carbon steels to achieve high strength and ductility should be as follows, wt.%: C = 0.30…0.55; Mn = 0.40…1.20; Si = 0.30…0.60.

In order to achieve the required indicators of physical and mechanical properties for alloying, microalloying and modification of base steels, it is advisable to use the following chemical elements: for alloying and microalloying — titanium, niobium, chromium and vanadium, for modification — nitrogen and rare earth metals on a cerium basis.

Taking into account the interaction of chemical elements in the C-Si-Mn system, to determine the optimal chemical composition of steels that can provide the required level of physical and mechanical properties of the metal of cast modules and their corrosion resistance in various aggressive environments, the effect of changing the content of the main chemical elements within the following limits was studied: carbon – from 0.25% to 0.60%, silicon – from 0.30% to 0.90%, manganese – from 0.50% to 2.0%. The content of phosphorus and sulfur did not exceed 0.045% of each element. The nitrogen and vanadium content was calculated for each steel grade taking into account that the equilibrium temperature of dissolution (separation) of the vanadium nitride phase in a solid solution does not exceed 1030°C [16].

Previous studies conducted at the Physico-Technological Institute of Metals and Alloys of the NAS of Ukraine on the influence of microalloying and modification processes with vanadium and nitrogen on the properties of structural steels of the C-Si-Mn-Cr system of ferritic-pearlitic and pearlitic classes have established that the separation of dispersed particles of VN and AIN in a solid solution provides a comprehensive increase in the strength and plasticity characteristics of steels to the level of properties of steels alloyed with molybdenum, nickel, niobium, vanadium, etc.

In this case, the process of dispersion strengthening of steel is implemented during the tempering of the product after normalization or quenching, which should occur at temperatures 100...150°C lower than the equilibrium temperature of dissolution (formation) of the vanadium nitride (VN) phase.

According to the results of previous studies, 35KhGAFL steel was selected, which has the highest indicators of casting and physical and mechanical properties for casting the above-mentioned protective modules [17–21].

Based on thermodynamic calculations of the equilibrium temperature of formation of the nitride disodium phase in a solid solution, it was established that the optimal range of austenitizing heating of 35KhGAFL steel during normalization and quenching is 920–940°C with holding for 1 hour.

After normalization, the samples were cooled in air, and during quenching – in water. Tempering was carried out at temperatures of 510–600°C with holding for 1 hour and subsequent cooling in air. Physical and mechanical properties were determined after normalization, quenching and tempering (**Table 4.1**).

After normalization (austenization), a fine-grained structure is observed in 35KhGAFL steel samples: 6–7 points and 7–8 points, respectively. The choice of heat treatment modes allows to provide the necessary set of steel properties depending on the operating conditions of protective structures.

To reduce the cost of casting and energy consumption, it is recommended to carry out normalization at 930°C with air cooling. The properties obtained under this mode fully comply with the technical requirements, and the grain size of the steel is 7–8 points, which indicates an optimal fine-grained structure [20].

The microstructures of steels after normalization and tempering are shown in **Fig. 4.5.** The microstructure of 35KhGAFL steel after normalization at a temperature of 930°C is pearlitic-ferritic: pearlite is thin-lamellar, ferrite is located outside the austenite grains in the form of broken meshes. Tempering of steel after normalization contributes to an increase in hardness due to the dispersion segregation of the vanadium nitride phase inside the grains.

Table 4.1 Heat treatment modes and physical and mechanical properties of 35KhGAFL steel

Heat treatment modes		Physical and mechanical properties of steel				
normalization, quenching °C, cooling medium	$\sigma_т$, MPa tempering °C	$\sigma_в$, MPa	ψ, %	KCU, J/cm^2	Hardness, HRC	
	no less than					
normalization at a temperature of 930°C, air	without tempering	600.0	850.0	22.0	72.0	20.0
	510	600.0	850.0	24.0	82.0	22.5
	550	600.0	890.0	24.0	82.0	22.0
	600	605.0	915.0	23.0	67.0	25.0
quenching from a temperature of 930°C, water	510	1010.0	1150.0	20.0	75.0	31.0
	550	795.0	980.0	27.0	84.0	26.0
	600	850.0	1010.0	24.0	75.0	26.0
Requirements according to the technical specifications		450…750	550…900	15…30	55…75	≥15

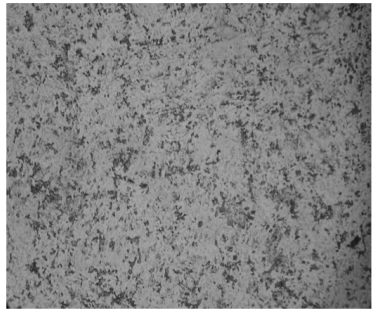

a

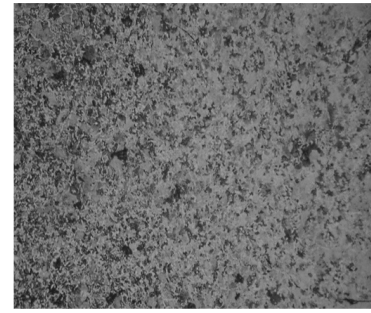

b

Fig. 4.5 Microstructures of the experimental 35KhGAFL steel after normalization at a temperature: *a* — of 930°C; *b* — normalization at a temperature of 930°C + tempering at a temperature of 510°C; ×200

Another urgent task during the production of castings using the lost foam casting process is to determine the level of non-metallic inclusions of medium and large sizes in the metal of the products. It is important to know not only the level of contamination of the metal with non-metallic inclusions, but also their morphology, size, shape and reasons contributing to their formation. In this case, it will be possible to use certain technological measures that will reduce their number or change their shape, for example, convert non-metallic inclusions from an acute-angled shape to a globular one, which will significantly increase the physical and mechanical properties of the metal.

The metal contamination index by non-metallic inclusions was determined by the linear method according to the requirements [21, 22] on unetched sections made from steel blanks. The results of the numerical values of each type of non-metallic inclusions and the total metal contamination index are given in **Table 4.2.**

Table 4.2 Metal contamination index of multifunctional modules by non-metallic inclusions of different morphology and the total contamination index

No.	Type of non-metallic inclusions	Contamination index of 35KhGAFL steel
1	Nitrides	0
2	Oxides	0.001127
3	Silicates	0.000407
4	Sulfides	0.008800
5	Total steel contamination index	0.002414

Analysis of the obtained results of the study of non-metallic inclusions in the recommended 35KhGAFL steel allowed to establish that the general index of contamination of the cast metal of samples cut from real modules made using polystyrene foam patterns is at the level of indicators for the metal of carbon steel products obtained using traditional casting technologies in one-time volumetric sand-clay molds [23].

Relatively large non-metallic inclusions of an oxide nature are observed in 35KhGAFL steel. Their appearance may be due to the presence of slag particles, since the samples were cut from the upper part of the cast module, or as a result of secondary oxidation of the melt during pouring the molds.

The heat treatment modes of the recommended steel do not significantly affect the morphology and number of non-metallic inclusions, with the exception of the normalization process. Prolonged cooling of the metal in air contributes to a partial redistribution of morphological types of inclusions – in particular, the proportion of sulfides increases, which is explained by a decrease in the solubility of sulfur in iron with a decrease in the temperature of the metal.

Based on the conducted studies, the optimal heat treatment regime is one that involves quenching from a temperature of 930°C in water with subsequent tempering at 510°C.

After such treatment, the steel is characterized by the following properties:

– tensile strength σ_v – not less than 1150 MPa;

– yield strength σ_t – not less than 1010 MPa;

– relative elongation δ – 16%;

– relative narrowing ψ – 20%;

– impact toughness KCU – 70 J/cm^2;

– hardness – 31 HRC.

The results obtained confirm that 35KhGAFL steel provides increased strength and ductility combined with good castability, which is crucial for the manufacture of thin-walled hollow elements of complex geometry [24].

4.3 DETERMINATION OF THE REINFORCEMENT INFLUENCE ON THE HYDRODYNAMICS OF MOLD FILLING AND THERMAL PROCESSES IN THE FUNCTIONAL FILLER

The influence of reinforcing steel elements and reinforcement directly from the liquid alloy of the shell on the hydrodynamics of mold filling and thermal processes in the functional filler was determined using computer simulation. Successful computer simulation can help reduce the number of tests and reduce the time for developing new castings due to a better understanding of the complex mechanisms and interaction of various technological parameters in the mold filling process, especially in the gasified pattern casting process [25, 26]. In accordance with the tasks of implementing technologies for obtaining lightweight high-strength steel hollow structures with non-metallic and metallic functional filler, the following types of them were proposed:

1 – steel shell filled with non-metallic functional material;

2 – steel shell with non-metallic functional material, which is reinforced with metal elements that simultaneously combine the shell and functional material;

3 – steel shell with non-metallic functional material, which is reinforced by solidification in its channels of liquid alloy of the shell, which at the same time combines the shell and functional material.

Computer simulation of the processes of pouring and solidification of the lost foam casting was performed using the Procast software. 3D drawings of the cell model of one element of the module (**Fig. 4.6**), gating system, reinforcement, core (functional filler) built in the CAD system were saved in IGES format and loaded into the simulation program. The element size when applying the mesh to the model, core and reinforcement was set to 2 mm. The total number of calculated elements was 739 thousand. The following materials were set from the database: Steel AISI 1040 – for the alloy, Sand LFC – for the ~~g~~ mold, Foam 30 kg/m^3 – for the model, Resin bonded sand permeable – for the core, Chill Carbon steel – for the reinforcement. The pouring temperature of the steel was set at 1580°C, the initial temperature of the mold, core, model and reinforcement, and the environment was 20°C. The heat transfer coefficients were set as follows: between liquid metal and foam – FOAMHTC 840, FOAMHTCMAX 10460, between liquid metal and mold/core – 500, between metal and reinforcement – 3000, between mold and core – 400. The boundary conditions were: inlet pressure on the upper surface of the riser 1.05 atm, temperature 1580°C, pressure around the mold 1 atm [9].

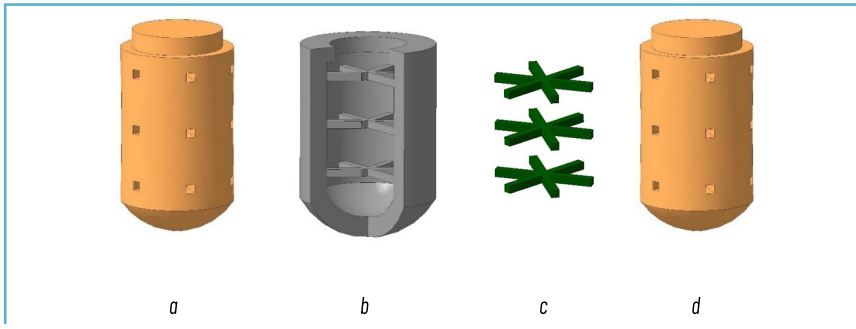

Fig. 4.6 General view of 3D models: *a* – cell; *b* – cell with membranes; *c* – reinforcement, *d* – core with channels

Fig. 4.7 shows the process of pouring an experimental cell with a functional filler without reinforcement. Under these conditions, the metal front moves from top to bottom with gradual spreading to the sides and the closing of two flows in the part opposite the supply point. In the case of the presence of polystyrene foam elements between the walls of the cell as a functional material, the nature of pouring is similar (**Fig. 4.8**). The presence of processes of filling thin channels of membranes (4x4 mm) is distinctive. Since the metal fills the cylindrical part of the cell, the metal enters each "beam" of the membrane from the main wall and moves to the point of their intersection.

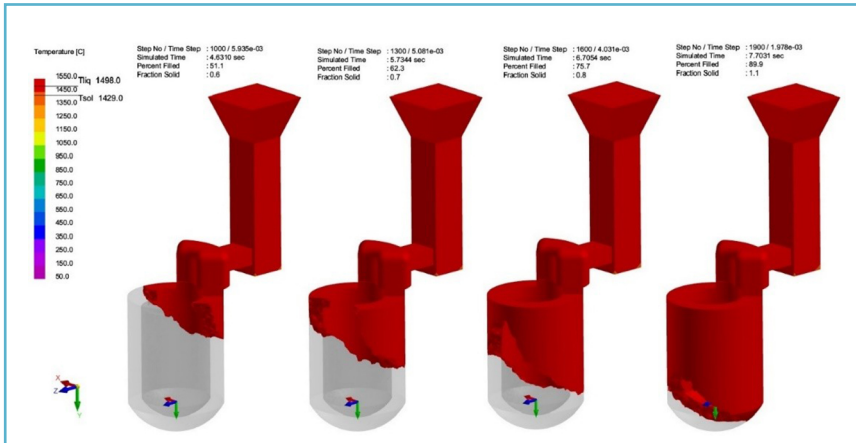

Fig. 4.7 The process of pouring an experimental cell (without reinforcement)

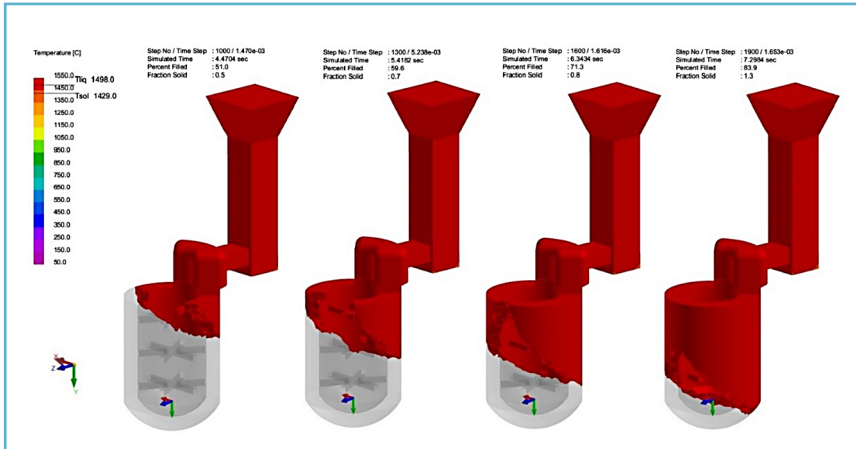

Fig. 4.8 The process of pouring an experimental cell with thin channels for reinforcement

The flow rate of liquid metal in the channels for reinforcement is shown in **Fig. 4.9.** At the beginning of filling the upper channel, the flow rate is about 2 cm/s. Then the speed increases to 4 cm/s. At the end of filling the channel, the speed briefly rises to 8 cm/s.

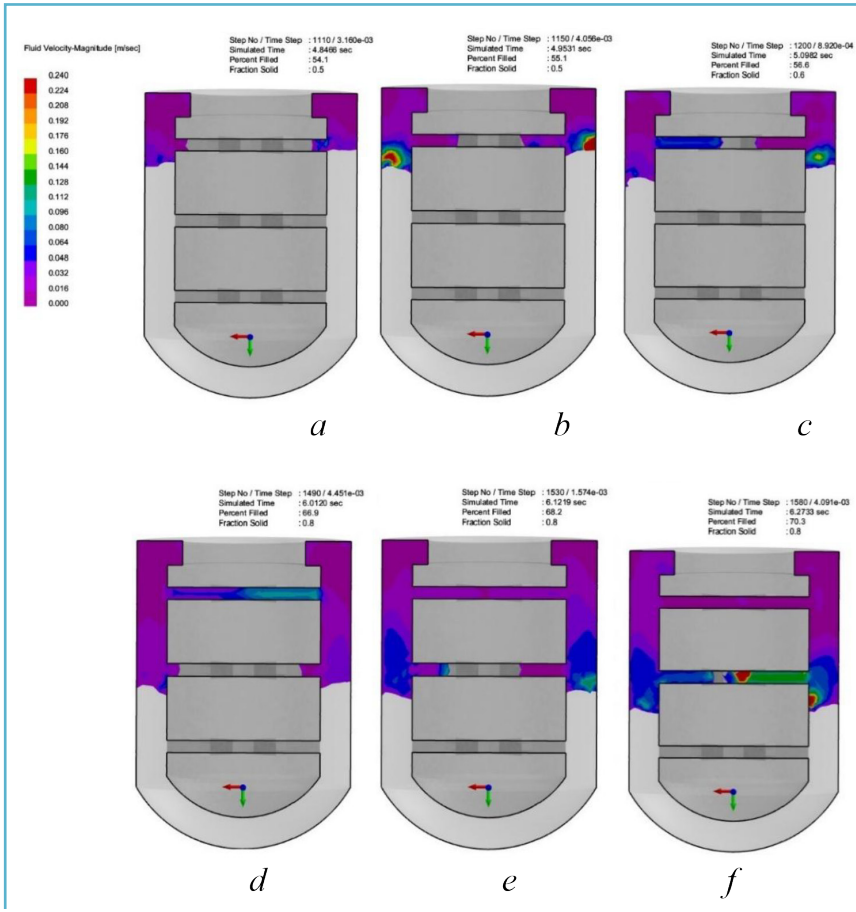

Fig. 4.9 The flow rate of liquid metal in the channels of the functional filler: *a* – 4.8 s, *b* – 5.0 s, *c* – 5.1 s, *d* – 6.0 s, *e* – 6.1 s, *f* – 6.3 s

A similar picture occurs when filling the middle and lower partitions. At the beginning of filling the channels, the speed is 2–3 cm/s. Then the speed increases to 6 cm/s, and briefly rises to 10–12 cm/s. It is believed that the optimal speed is 3–4 cm/s. When the metal moves through thin channels, a high speed contributes to their filling, since at a low speed the flow may stop due to its cooling.

Fig. 4.10, *a* shows the temperature fields of the longitudinal section of a casting with a functional filler, a casting with a functional filler and reinforcement (**Fig. 4.10, *b***), a casting with membranes and a functional filler (**Fig. 4.10, *c***).

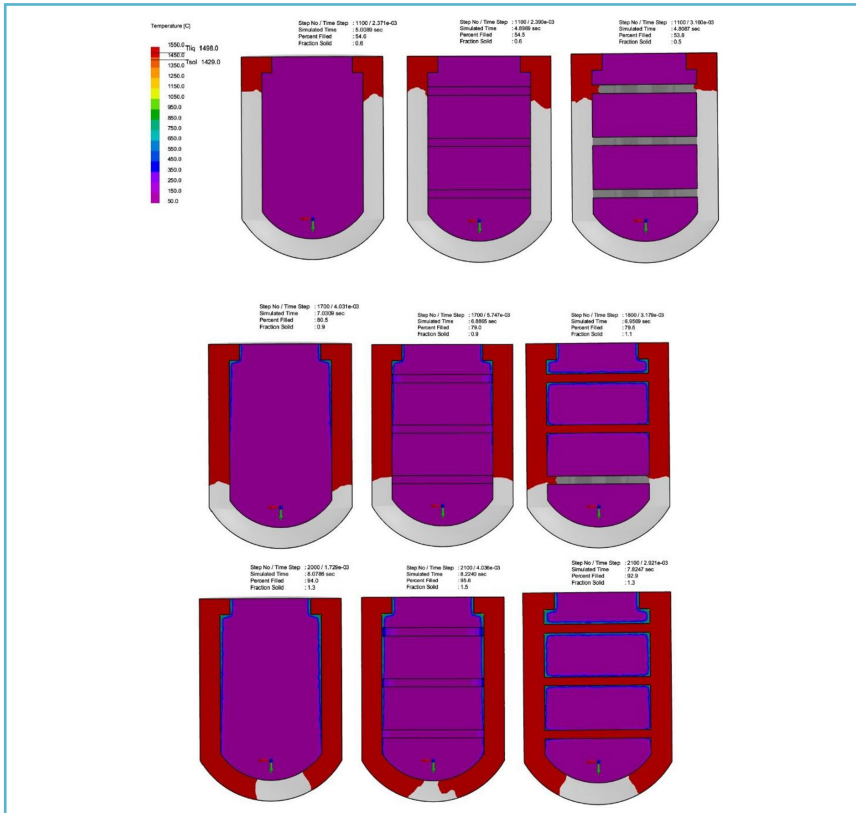

Fig. 4.10 Temperature fields (cell cross-section) during pouring: *a* – casting with functional material; *b* – casting with reinforced filler; *c* – casting with functional filler reinforced from the liquid phase of the shell metal

The nature of filling the casting cavity for the first two cases is the same. In the third variant, the nature of filling is somewhat different, which is associated with the presence of partitions. During pouring, the functional material is heated only in the contact zone to approximately 400°C. At the end of pouring, the upper part of the functional filler is heated to a depth of up to 2 mm to a temperature of 700°C.

Fig. 4.11 shows the temperature fields of the longitudinal section of the casting during solidification and cooling of the metal. **Fig. 4.12** shows the solidification time of the section of the castings. 30 seconds after filling the casting, the functional filler is heated to a depth of up to 7 mm. Complete heating of the

functional filler in the first variant occurs in 180 s, in the variant with reinforcement — in 130 s, in the variant with reinforcement from the liquid phase of the shell metal — in 100 s.

The highest temperature to which the functional filler is fully heated in the first case is 850°C, in the case of using reinforcement — 1050°C, in the case of casting with membranes — 1150°C. Thus, the best conditions for sintering the functional filler are created in the second two variants.

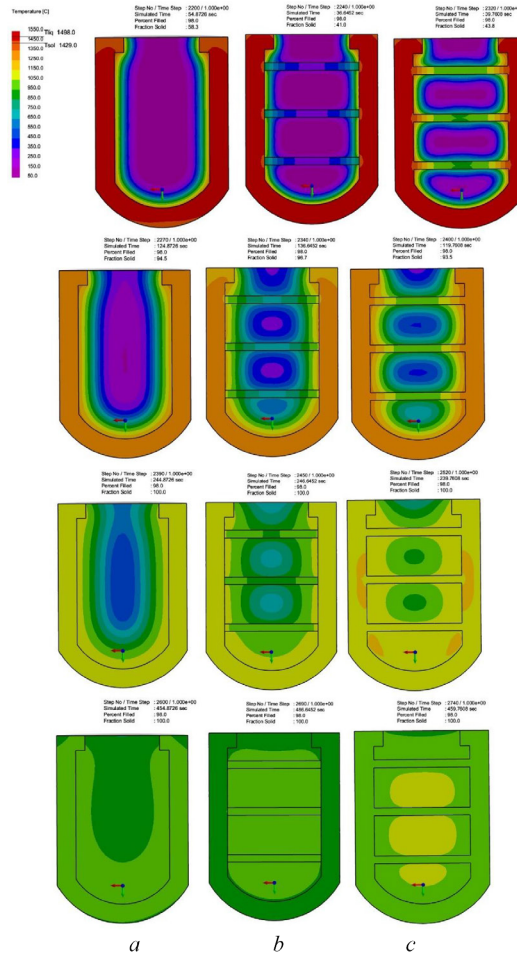

Fig. 4.11 Temperature fields (cell cross-section) during solidification and cooling: *a* — casting with functional material; *b* — casting with reinforced functional material; *c* — casting with functional filler, which is reinforced from the liquid phase of the shell metal

The presence of reinforcement or membranes affects the solidification processes (**Fig. 4.12**). The reinforcement acts as a refrigerator and reduces the solidification time of the casting by 11 s. The membranes harden quite quickly (12 s) and partially cool the casting, but reduce the solidification time of the casting by only 6 s.

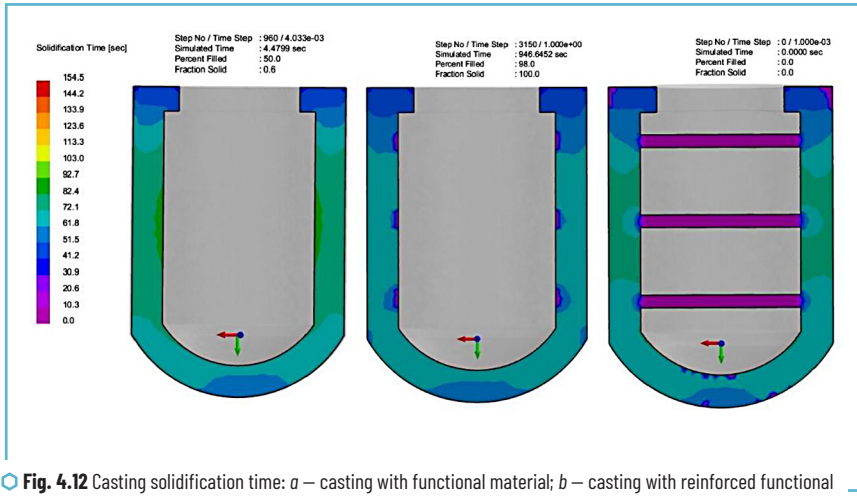

Fig. 4.12 Casting solidification time: *a* — casting with functional material; *b* — casting with reinforced functional material; *c* — casting with functional filler, which is reinforced from the liquid phase of the shell metal

The nature of filling the cell without membranes, determined on the basis of simulation, is typical for the upper feed for lost foam casting due to the presence of a polystyrene foam pattern, which exerts thermomechanical resistance. In the presence of membranes, significant changes in the nature of filling the main wall of the cell do not occur, due to the fact that the volume of the membranes is 3.5% of the total volume of the cell. However, the metal flow rate in the membranes is 3–4 times higher than the metal flow in the cavity of the main wall of the casting, which is due to hydrodynamic pressure.

The results of the study of the temperature fields of the casting and the functional filler during pouring, solidification and cooling of the metal showed that when using reinforcement and the presence of metal membranes, better conditions are created for sintering the functional filler due to the heat of the matrix metal.

The increase in the heating rate of the functional filler in the presence of steel reinforcement is associated with the higher thermal conductivity of the steel, which is heated by the heat of the casting. In the case of a casting with membranes, they increase the area of the contact surface for heat exchange of the metal with the functional filler. In addition, the casting with membranes has a larger mass, respectively, the amount of heat transferred by the matrix metal to the functional filler increases.

Reducing the hardening time, i.e. increasing the hardening rate, creates conditions for increasing the mechanical properties of the casting.

In addition to the hardening rate, the level of mechanical properties of steel is affected by the presence of casting defects, so the work analyzed the shrinkage that is formed in the cell casting. The shrinkage fields of the first and third types of shells are presented in **Fig. 4.13.** The simulation results showed that in a casting without partitions, shrinkage is concentrated in the pouring part. At the same time, in a casting with a filler, which is reinforced from the liquid phase of the shell metal, shrinkage cavities are also present in the center of the partitions. This is explained by the formed "thermal node", which occurs when six "beams" are connected, which solidifies without being fed with liquid metal from the main walls of the shell or pouring.

To prevent shrinkage in the center of the partitions, another design was proposed, in which the central part has the shape of a ring. The simulation results of the solidification of this version of the casting **(Fig. 4.14)** showed that there is a certain porosity in the partitions (reinforcement formed from the liquid phase of the shell metal). However, the size of the shrinkage defects has significantly decreased compared to the previous version.

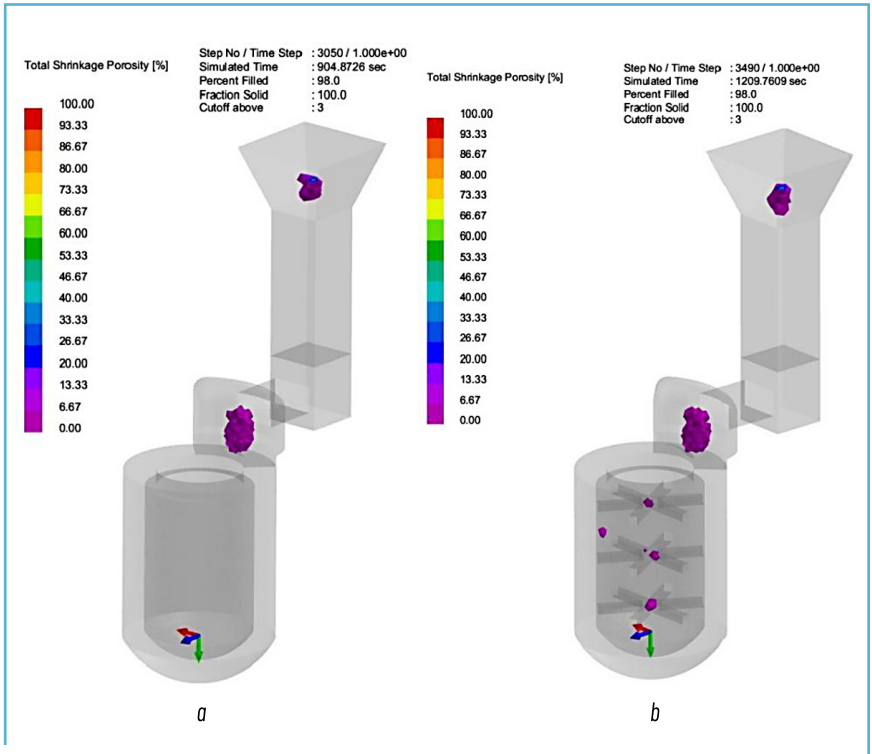

Fig. 4.13 Shrinkage fields: *a* — casting with functional filler; *b* — casting with functional filler reinforced from the liquid phase of the shell metal

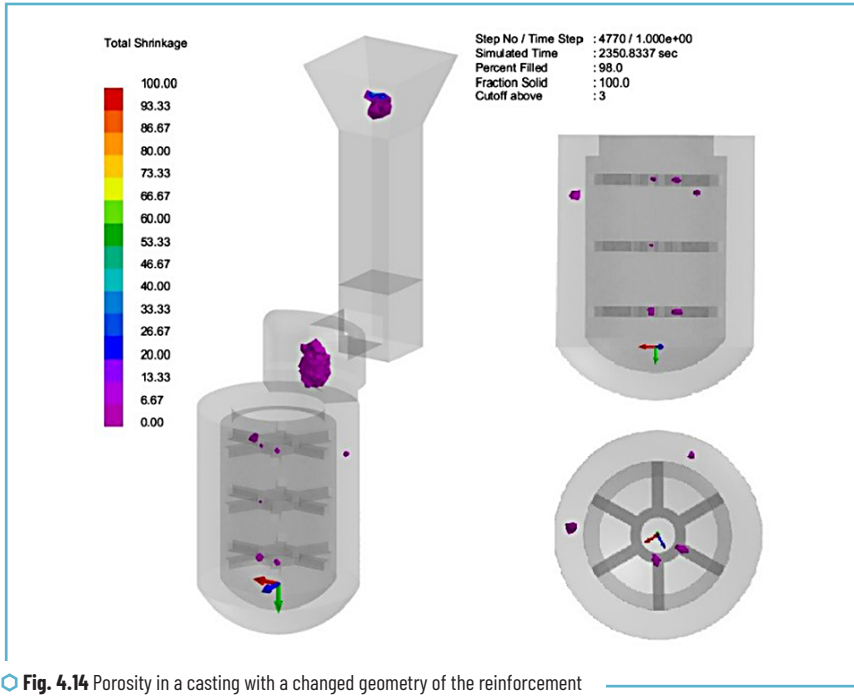

Fig. 4.14 Porosity in a casting with a changed geometry of the reinforcement

Thus, the conducted studies have shown the feasibility of using solid reinforcement and reinforcement from liquid metal to increase the mechanical adhesion of the shell metal with the functional filler and create better conditions for its sintering for the purpose of strengthening.

4.3.2 STUDIES ON THE SELECTION OF A FUNCTIONAL FILLER

The functional filler of the metal shell must satisfy several parameters – availability, low mass, refractoriness, etc. At the same time, the filler must have sufficient hardness to resist the penetration of objects (fragments, bullets, etc.) into them, and have a low density so as not to significantly increase the total mass of the protective module.

The properties of some common materials (**Table 4.3**) that can be used as fillers are analyzed. The most accessible and cheap is quartz sand, which has a sufficiently high refractoriness and hardness, is characterized by a small bulk mass. Electrocorundum and silicon carbide are more refractory and hard, but they are more expensive and have a higher density. An accessible material that has a low bulk density is expanded vermiculite, but is characterized by low refractoriness and low hardness.

Table 4.3 Characteristics of non-metallic fillers

No.	Name	Chemical formula	Density, kg/m^3	Bulk weight, kg/m^3	Melting temperature (fire resistance), °C	Mohs hardness
1	Crystalline quartz (quartz sand)	SiO_2	2650	1400–1700	1713 (1650)	5.5–7.0
2	Electrocorundum	Al_2O_3	3990	2400	2050	9.0
3	Expanded vermiculite	$(Mg, Fe^{2+}, Fe^{3+})_3 [(OH)_2 (Al, Si)_4 4H_2O$	380	200	~1300	1.0–1.5
4	Silicon carbide	SiC	3210	1900	2730	9.5

For practical testing of the behavior of functional fillers in combination with the shells of protective structures, cylindrical samples were filled with different fillers. Polystyrene cylinders were made – outer diameter 66 mm, inner 40 mm, height 50 mm. As fillers, quartz sand of fraction 0.16–0.2 mm, fraction 0.8–1.0 mm, expanded vermiculite of fraction 1.0 mm, normal electrocorundum of fraction 0.8 mm (F24) were used. Liquid glass was used as a binder, which was added in an amount of 7% by weight of the core mixture.

8 samples of models with different fillers were made (**Fig. 4.15**):

1 – quartz sand of fraction 0.16–0.2 mm;

2 – a mixture of vermiculite and quartz sand of fraction 0.16–0.2 mm;

3 – quartz sand of fraction 0.16–0.2 mm mixed with aluminum shavings;

4 – quartz sand of fraction 0.8–1.0 mm;

5 – quartz sand of fraction 0.8–1.0 mm mixed with polystyrene granules;

6 – quartz sand of fraction 0.8–1.0 mm with polystyrene foam membranes;

7 – vermiculite;

8 – normal electrocorundum.

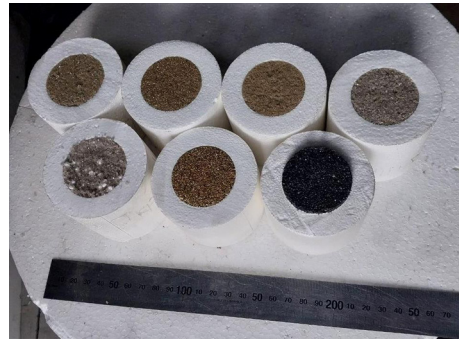

Fig. 4.15 Cylindrical samples with different fillers

The core mixtures were obtained by mixing the components until the refractory particles were completely "wetted" with liquid glass. Then the mixture was "stuffed" into the cylinder hole and left for 24 hours in a warm room to cure and dry the mixture. After that, the elements of the gating system were glued and a refractory coating was applied (**Fig. 4.16, *a*).** After the coating dried, the pattern blocks were molded in dry quartz sand using the traditional LFC technology. The molds were poured with liquid steel 45L. After the castings cooled, they were knocked out of the mold (**Fig. 4.16, *b***) and separated from the sprues (**Fig. 4.17**).

a *b*

Fig. 4.16 Samples: *a* — pattern blocks; *b* — casting bushes

Fig. 4.17 Cast samples with different fillers

To study the interaction of fillers with the shell metal, a longitudinal section of the cylinders was performed (**Fig. 4.18–4.20**). Samples with quartz sand were characterized by metal penetration to a depth of 1 mm, and samples with a mixture of vermiculite and quartz sand — to a depth of 2—3 mm. Aluminum chips, which were added to the sand to "bind" the sand grains, melted only in a 5 mm thick layer adjacent to the shell metal.

Coarse sand had larger porosity between the sand grains, which should contribute to better metal penetration. However, no significant increase in the penetration depth was observed, only within 1–2 mm. In the filler with the addition of polystyrene foam granules, the thickness of the penetration layer increased to 3 mm, but the cavities formed after the polystyrene foam granules burned out did not fill with metal. Moreover, the formed cavities reduced the filler's resistance to spalling. When using polystyrene foam membranes, the shell metal penetration layer into the filler increased to 3–4 mm.

Samples with expanded vermiculite had shells and were characterized by significant defects. This is explained by the low fire resistance of this filler. Because of this, the mixture with vermiculite also had high spalling.

In samples with electrocorundum filler, the penetration layer was 1–2 mm. These samples were also characterized by average spalling. The reason for this is that the material used consists of particles of the same fraction. For example, quartz sand by its nature consists of particles of different sizes. In this case, the binder creates more bonds, since small grains are located between large ones. Therefore, to increase the strength of corundum fillers, it is necessary to mix several fractions to get more bonds in the mixture. Also, samples with corundum had a greater mass than samples with quartz sand.

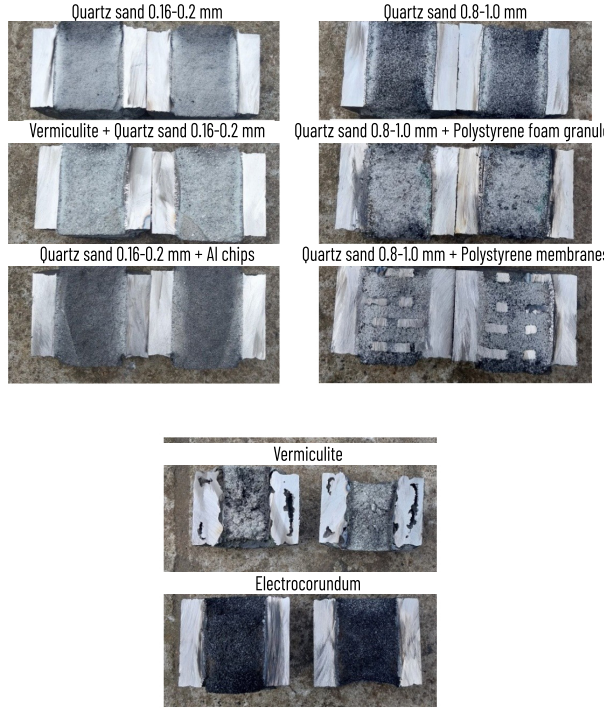

Fig. 4.18 Sections of cast samples with fillers

Fig. 4.19 Sections of cast samples with different fillers

Fig. 4.20 Section of samples with quartz sand filler and membranes obtained by liquid-phase reinforcement

The conducted studies have shown that a mixture of quartz sand with liquid glass is the most suitable functional filler for shell modules. Adding vermiculite to quartz sand may also be promising in order to reduce the mass of the cast module. The use of reinforcement of the filler from the liquid phase of the shell contributed to an increase in the metal penetration layer and the formation of a metal composite.

4.3.3 DEVELOPMENT OF TECHNOLOGY FOR MANUFACTURING MODULE CASTING

Taking into account previous experience in obtaining similar castings, a gating-feeding system was developed, the general view of which is shown in **Fig. 4.21,** for a 500x500 mm module casting. The lower metal supply was selected to ensure uniform filling and uniform gasification of the pattern. To compensate for shrinkage, a riser was placed above the casting.

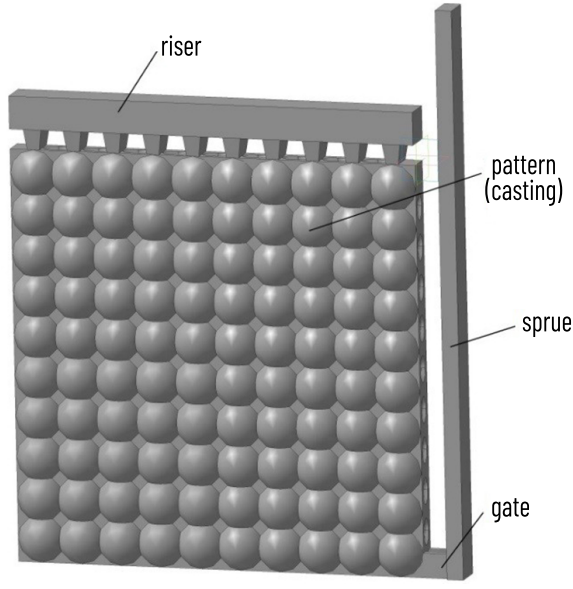

Fig. 4.21 General view of the gating system

Simulation of the pouring and solidification processes of the module casting by lost foam casting was performed using the Procast software.

The parameters necessary for simulation — the properties of 45L steel, polystyrene foam and quartz sand — were selected from the database. The pouring temperature of the steel was set to 1580°C, the initial temperature of the mold — 20°C.

The results of the simulation of pouring a casting of a module 500x500 are shown in **Fig. 4.22**. The total pouring time is 45 s. Filling occurs from one side of the gates. The metal front moves from right to left and from bottom to top simultaneously. This nature of pouring is due to the thermomechanical resistance of the polystyrene foam pattern.

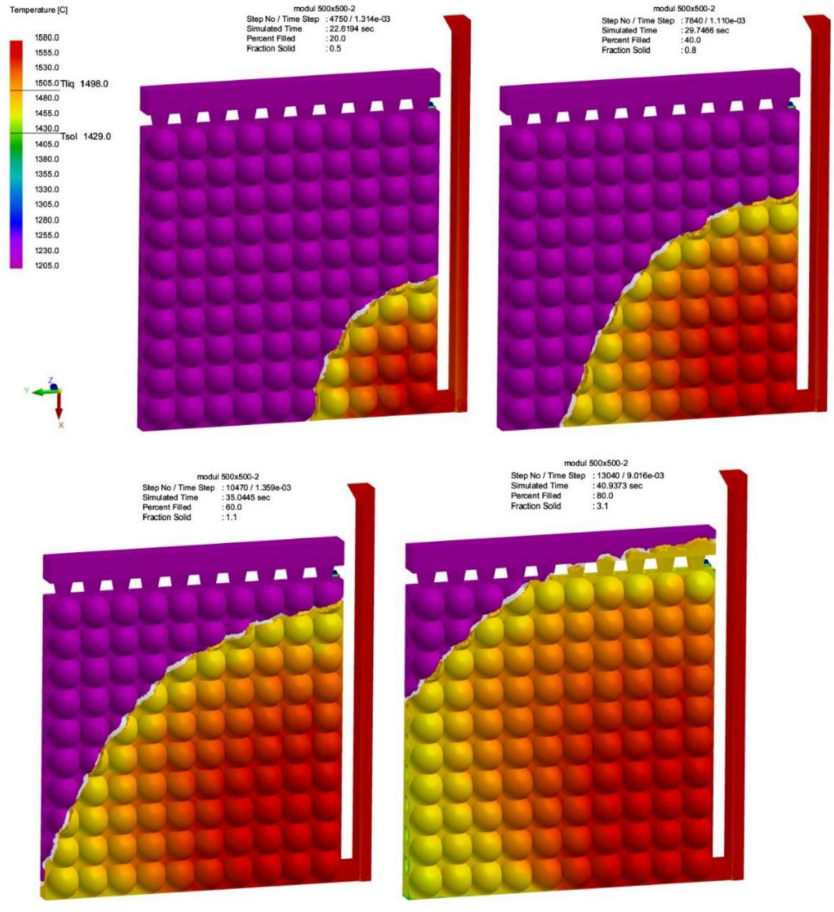

Fig. 4.22 Hydrodynamics of pouring a casting of a module 500x500

An important parameter of the pouring process that affects the formation of casting defects is the melt velocity in the mold. Therefore, the melt flow velocity when filling the casting cavity was investigated.

As the simulation results show (**Fig. 4.23**), the melt front velocity is within 3–5 cm/s throughout the entire pouring time. In the gate and the cell near it, the flow velocity reaches a value of 15 cm/s, which is due to the hydrodynamic pressure created by the metal in the sprue.

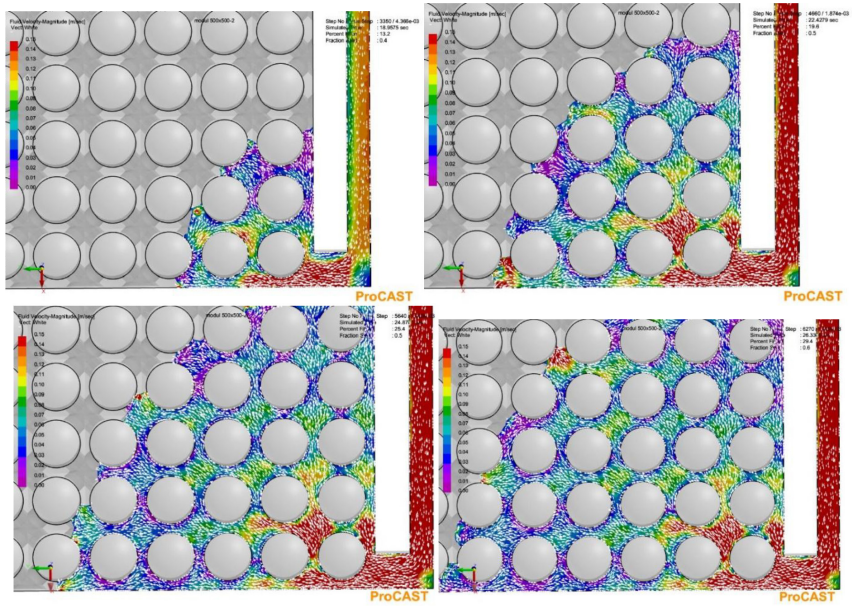

Fig. 4.23 Melt velocity during pouring of the casting

The results of simulation the solidification process of the casting showed that the solidification of the casting body occurs almost uniformly (within 60–90 s) (**Fig. 4.24, *a***). The solidification time of the riser is twice as long, which contributes to the feeding of the walls of the casting with liquid metal from it. The sprue solidifies last, since it contains the hottest metal, and the layers of molding sand around it heat up during pouring, respectively, the temperature gradient between the sprue metal and the mold decreases, slowing down the solidification rate. As a result, shrinkage is concentrated in the riser and the sprue (**Fig. 4.24, *b***).

The porosity in the casting was also studied. The simulation results demonstrated (**Fig. 4.25**) that the porosity of a shrinkage nature is absent in the casting body.

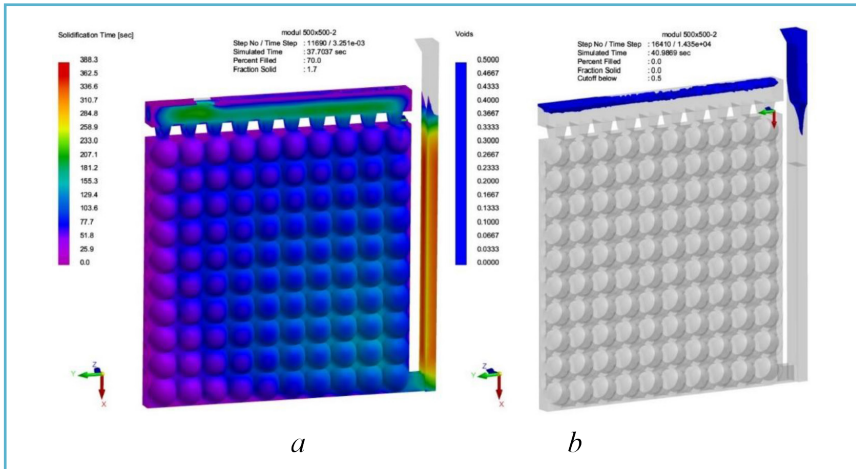

Fig. 4.24 Module casting: *a* — solidification time; *b* — shrinkage

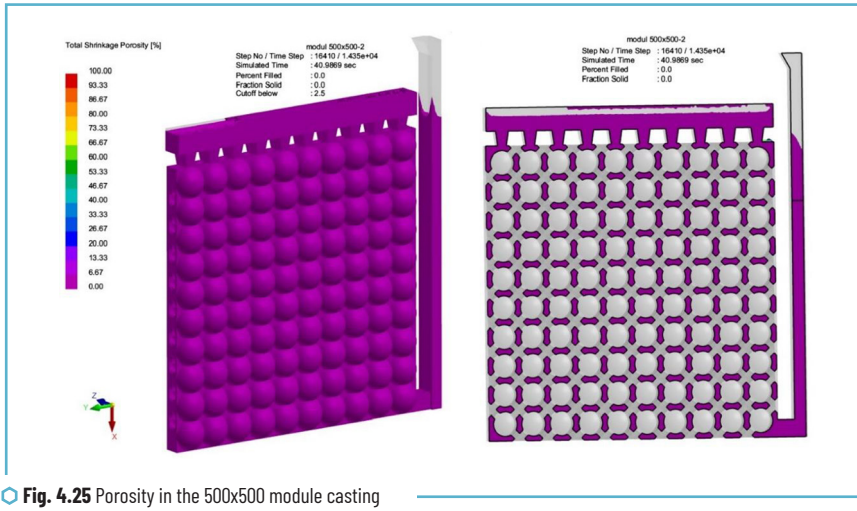

Fig. 4.25 Porosity in the 500x500 module casting

The gating system developed in this way ensures gradual and uniform gasification of the polystyrene foam pattern, contributing to the removal of destruction products from the mold. The melt front velocity of 3–5 cm/s contributes to the rapid replacement of the pattern, but allows to avoid the "coverage" mode of the pattern and the formation of gas defects due to this. During solidification, due to the equilaterality, the casting solidifies almost simultaneously, and shrinkage cavities are concentrated in the riser.

4.3.4 VERIFICATION OF THE TECHNOLOGICAL PROCESS

To verify the technological process of manufacturing hollow cast structures with composite and reinforced non-metallic functional filler from developed steels according to LFC, laboratory and experimental verifications of calculations, simulation and the developed route technological process were carried out.

In this test evaluation, the developed methods for calculating basic parameters and a set of technological divisions, types and characteristics of materials, limits of variation in the parameters of the technological processes of obtaining polystyrene foam patterns, reinforcing composite, preparation and application of refractory coatings on these patterns, as well as pouring the mold and obtaining castings were subject to the developed test evaluation. A casting drawing was previously developed and a pattern was cut out of an EPS 150 (PSB 25–30) polystyrene board on a 3D milling machine, the cavity of which was filled with a reinforcing mixture (**Fig. 4.26**).

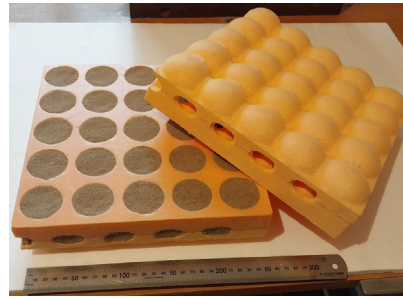

Fig. 4.26 Polystyrene foam pattern of the protective module

In the following, the stages of the technological process were sequentially performed, steel of the required chemical composition was melted and high-quality castings were obtained (**Fig. 4.27**).

Fig. 4.27 Reinforced steel castings of the protective module, which were manufactured using the developed technology

Thus, the created technological processes for obtaining hollow cast structures with composite and reinforced non-metallic functional filler from developed steels using LFC make it possible to obtain reinforced structures that can be used in protective structures.

CONCLUSIONS

Based on the mechanism of interaction of matrix alloy (MA) in the mold in the presence of metal reinforcing elements with polystyrene foam pattern and thermal destruction products in the form of liquid, gaseous and solid phases, a computational model of heat and mass exchange processes was developed with the determination of the heat transfer coefficient in the criterion form (based on the Nusselt, Prandtl, Reynolds criteria) for the flow of liquid MA in the mold.

The task of developing a technological process for obtaining lightweight high-strength steel hollow structures with a non-metallic functional filler, which is a binary part of a single structure and counteracts impact dynamic loads upon contact with high-speed bodies, was solved. Additional reinforcement was carried out in the systems "metal shell – functional filler – solid reinforcing phase or reinforcing phase formed from liquid shell metal", which has not yet been studied in the theory of foundry production, and therefore there are no analogues.

According to the results of research on the features of the hydrodynamic conditions for filling the mold cavity with liquid steel and in the presence of a solid reinforcing phase and thin channels formed in the functional filler, it was established that the time for filling the mold cavity is 7.5...8.0 s for all types of objects under study and the metal flow rate in the thin channels of the filler is 5..7 cm/s, which are optimal for obtaining steel shells when lost foam casting.

The presence of solid metal reinforcement and liquid, solidifying metal of the shell in its thin channels placed in the functional filler affects the heat and mass transfer processes in the mold. Thus, with intensive heating of the functional material due to heat transfer from the reinforcing phase, the functional material heats up during the solidification of the metal shell to a temperature of 1050°C in 130 s (solid state) and during the formation of the reinforcing phase from the shell metal to 1150°C in 100 s. Under such thermophysical conditions, the possibility of sintering (melting) of the non-metallic (metallic) functional layer around the reinforcing phase is created and thereby significantly additionally enhances the operational characteristics of the binary module structure.

It is also determined that the filling of the shell in the thin channels formed in the functional material occurs when pouring metal, which guarantees the specified geometric dimensions of the reinforcing phase and, accordingly, its mechanical properties, which also enhances the operational parameters of the binary module structure.

It was determined that a mixture of quartz sand with liquid glass is the most acceptable functional filler for shell modules. Adding vermiculite to quartz sand may also be promising in order to reduce the mass of the cast module. The use of filler reinforcement with the liquid phase of the shell contributed to an increase in the metal penetration layer and the formation of a metal composite.

According to the results of research on the selection of the optimal chemical composition of steels with specified mechanical properties for hollow structures for the construction of various types of modular protective structures, 35KhGAFL steel with the chemical composition, wt.%: C = 0.30…0.40; Mn = 0.60…0.90; Si = 0.55…0.65; Cr = 0.20…0.70; N = 0.012…0.015; V = 0.08…0.11; S and P ≤ 0.025 of each element; Al = 0.015…0.025. It was established that the best set of mechanical properties for 35KhGAFL steel can be achieved after quenching from a temperature of 930°C in water and tempering at a temperature of 510°C: σ_v = 1150 MPa, σ_τ = 1010 MPa, δ = 16%, ψ = 20%, KCU = 70 J/cm^2, hardness — 31 HRC.

Technological processes for obtaining hollow cast structures with composite and reinforced non-metallic functional filler from developed steels according to LFC have been created and tested, which make it possible to obtain reinforced structures, in particular for protective structures.

FINANCING

The research was carried out within the framework of the project No. state registration 0124U003980 with the support of a grant from the National Research Foundation of Ukraine under the program "Science for Strengthening the Defense Capability of Ukraine".

CONFLICT OF INTEREST

The authors declare that they have no conflict of interest in relation to this research, whether financial, personal, authorship or otherwise, that could affect the research and its results presented in this paper.

USE OF ARTIFICIAL INTELLIGENCE

The authors confirm that they did not use artificial intelligence technologies in creating the submitted work.

REFERENCES

1. Charchi, A., Rezaei, M., Hossainpour, S., Shayegh, J., Falak, S. (2010). Numerical simulation of heat transfer and fluid flow of molten metal in MMA—St copolymer lost foam casting process. Journal of Materials Processing Technology, 210 (14), 2071—2080. https://doi.org/10.1016/j.jmatprotec.2010.07.028
2. Narivskiy, A., Shinsky, O., Shalevska, I., Kvasnitska, Y., Kaliuzhnyi, P., Polyvoda, S. (2023). Modern technological processes of obtaining cast products and structures of responsible purpose from aluminum, ferrous carbon and heat-resistant alloys. Structural materials: manufacture, properties, conditions of use. Kharkiv: TECHNOLOGY CENTER PC, 32—67. https://doi.org/10.15587/978-617-7319-97-8.ch2

3. Shalevska, I. A. (2020) Complex of technological processes of ecologically safe production of lost-foam castings with predicted functional properties. [Doctoral dissertation; Physico-Technological Institute of Metals and Alloys of the National Academy of Science of Ukraine].
4. Kreith, F., Bohn, M. (1997). Principles of Heat Transfer. General Engineering Series. PWS Publishing Company, 793.
5. Shinsky, O. I. (1997). Gazogidrodinamika i tekhnologii litia zhelezouglerodistykh i tcvetnykh splavov po gazifitciruemym modeliam. [Doctoral dissertation; Physico-Technological Institute of Metals and Alloys of the National Academy of Science of Ukraine].
6. Narivskiy, A., Shinsky, O., Shalevska, I., Kvasnitska, Y., Kaliuzhnyi, P., Polyvoda, S. (2023). The influence of external actions and methods of alloying alloys on the operational characteristics of cast products. Structural materials: manufacture, properties, conditions of use. Kharkiv: TECHNOLOGY CENTER PC, 121–157. https://doi.org/10.15587/978-617-7319-97-8.ch4
7. Nagata, S., Sakamoto, M. (1989). Development and applications of metal composites from pressure casting. Materials & Design, 10 (3), 153–158. https://doi.org/10.1016/s0261-3069(89)80031-7
8. Wakai, E., Noto, H., Shibayama, T., Furuya, K., Ando, M., Kamada, T. et al. (2024). Microstructures and hardness of BCC phase iron-based high entropy alloy Fe-Mn-Cr-V-Al-C. Materials Characterization, 211, 113881. https://doi.org/10.1016/j.matchar.2024.113881
9. Shinsky, O., Kvasnytska, I., Shalevska, I., Kaliuzhnyi, P., Neima, O. (2024). Devising a technology for manufacturing hollow cast steel structures with composite and reinforced non-metallic functional filler. Eastern-European Journal of Enterprise Technologies, 6 (12 (132)), 6–14. https://doi.org/10.15587/1729-4061.2024.318553
10. Azeem Ullah, M., Cao, Q. P., Wang, X. D., Ding, S. Q., Abubaker Khan, M., Zhang, D. X., Jiang, J. Z. (2024). Carbon effect on tensile and wear behaviors for a dual-phase Fe61.5Cr17.5Ni13Al8 alloy. Materials Science and Engineering: A, 914, 147128. https://doi.org/10.1016/j.msea.2024.147128
11. Tsyganov, V., Naumik, V., Byalik, H., Ivschenko, L., Mokhnach, R. (2019). Steel-copper nano-composited materials. Contributed Papers from Materials Science and Technology 2019 (MS&T19). Portland, 439–443.
12. Kondratyuk, S. Ye., Veis, V. I., Parkhomchuk, Z. V., Kvasnytska, Y. H., Kvasnytska, K. H. (2024). Thermokinetic Parameters of Solidification and Gradient Structure of Steel Castings. Metallofizika i Noveishie Tekhnologii, 45 (7), 865–872. https://doi.org/10.15407/mfint.45.07.0865
13. Shalevska, I. A., Doroshenko, V. S., Kaliuzhnyi, P. B., Kvasnytska, Yu. G. (2022). Review of the use of cast metal materials in the construction of underground and protective structures. Metal and Casting of Ukraine, 30 (4), 54–61. https://doi.org/10.15407/steelcast2022.04.054
14. ASTM A732/A732M-20. Specification for Castings, Investment, Carbon and Low Alloy Steel for General Application, and Cobalt Alloy for High Strength at Elevated Temperatures. https://doi.org/10.1520/a0732_a0732m-20
15. Shypytsyn, S., Fedorov, H., Kirchu, I., Lykhovey, D., Stepanova, T. (2024). Increasing the physical-mechanical and operational properties of high manganese steels by improving the technological processes of their melting, micro-alloying and modification. Casting Processes, 155 (1), 14–28. https://doi.org/10.15407/plit2024.01.014

16. Yamshinsky, M. M., Fedorov, G. E., Radchenko, K. S. (2015). Termostiikist zharostiikykh stalei dlia roboty v ekstremalnykh umovakh. Visnyk Donbaskoi derzhavnoi mashynobudivnoi akademii, 3, 33—37.
17. DSTU 8781:2018. Steel castings. General specifications (2018). DP «UkrNDNTs». Available at: https://online.budstandart.com/ua/catalog/doc-page.html?id_doc=77524
18. Yamshinsky, M. M., Fedorov, G. E. (2015). Liteinye i mekhanicheskie svoistva zharostoikikh stalei. Lite i metallurgiia, 2, 17—24.
19. ISO 4990:2023. Steel castings — General technical delivery requirements. (2023). ISO. Available at: https://cdn.standards.iteh.ai/samples/84185/33d9639ba3db417ab01fe2a41751f295/ISO-4990-2023.pdf
20. DSTU 9074:2021. Steel. Microstructure Standarts (2021). DP «UkrNDNTs». Available at: https://online.budstandart.com/ua/catalog/doc-page.html?id_doc=94147
21. DSTU 8966:2019. Steel. Metalographic method for the determination of nonmetallic inclusions (2019). DP «UkrNDNTs». Available at: https://online.budstandart.com/ua/catalog/doc-page.html?id_doc=88067
22. ISO 643:1983. Steels — Micrographic determination of the ferritic or austenitic grain size (1983). ISO. Available at: https://cdn.standards.iteh.ai/samples/4773/6ad7e45fca0d4daa86654405f6e2d12e/ISO-643-1983.pdf [in English].
23. DSTU 7809:2015. Carbon Structural Quality Steel Gauged Bars With Special Surface Finish. General specifications (2015). DP «UkrNDNTs». Available at: https://online.budstandart.com/ru/catalog/doc-page?id_doc=64320
24. Shinsky, O., Fedorov, G., Kvasnytska, I., Shalevska, I., Kaliuzhnyi, P., Neima, O., Shalevskyi, A. (2025). Selection of materials for the manufacture of cast hollow metal modules of protective structures. Casting Processes, 159 (1), 11—21. https://doi.org/10.15407/plit2025.01.011
25. Liu, X. J., Bhavnani, S. H., Overfelt, R. A. (2007). Simulation of EPS foam decomposition in the lost foam casting process. Journal of Materials Processing Technology, 182 (1-3), 333—342. https://doi.org/10.1016/j.jmatprotec.2006.08.023
26. Kaliuzhnyi, P., Shalevska, I., Shynskyi, O. (2024). Casting of a Steel Valve Body Using Lost Foam Sand casting: Comparison Between Experimental and Simulation Results. International Journal of Metalcasting, 19 (4), 2409—2418. https://doi.org/10.1007/s40962-024-01487-2